

Article

Photocatalytic Duplex-Based DNazymes Switched by an Abasic Site

Longlong Gao , Rui Tian and Yong Shao *

Key Laboratory of the Ministry of Education for Advanced Catalysis Materials, College of Chemistry and Materials Science, Zhejiang Normal University, Jinhua 321004, China

* Correspondence: yshao@zjnu.cn; Fax: +86-579-8228-2595

Abstract: DNazymes have attracted increasing interest in developments of gene tools, therapies, and biosensors. Among them, G-quadruplexes are widely used as the key structure elements of DNazymes to activate the catalytic competency of specific cofactors, such as hemin, but there is a great demand to diversify DNazymes using other more straightforward DNA structures such as fully matched duplex (FM-DNA). However, the perfect base pairs in duplex limit the DNzyme activity. In this work, a photocatalytic DNzyme was developed by introducing an abasic site (AP site) into duplex (AP-DNA) to switch its photocatalytic activity. Palmatine (PAL), a photosensitizer from natural isoquinoline alkaloids, served as a cofactor of the DNzyme by binding at the AP site. The AP site provides a less polarized environment to favor the PAL fluorescence. As a result, dissolved oxygen was converted into singlet oxygen ($^1\text{O}_2$) via energy transfer from the excited PAL. The oxidation of substrates by the in situ photogenerated $^1\text{O}_2$ served as a readout for the DNzyme. In addition, the duplex-based DNzyme was engineered from FM-DNA by the cascade uracil-DNA glycosylase to generate AP-DNA. Our work provides a new way to construct duplex-based DNzymes.

Keywords: DNzyme; duplex; abasic site; photocatalysis; isoquinoline alkaloids; palmatine



Citation: Gao, L.; Tian, R.; Shao, Y. Photocatalytic Duplex-Based DNazymes Switched by an Abasic Site. *Chemistry* **2023**, *5*, 1497–1507. <https://doi.org/10.3390/chemistry5030102>

Academic Editor: Di Li

Received: 5 June 2023

Revised: 25 June 2023

Accepted: 26 June 2023

Published: 28 June 2023



Copyright: © 2023 by the authors. Licensee MDPI, Basel, Switzerland. This article is an open access article distributed under the terms and conditions of the Creative Commons Attribution (CC BY) license (<https://creativecommons.org/licenses/by/4.0/>).

1. Introduction

DNazymes have found wide applications including DNA/RNA cleavage, biodevices, and sensors [1–10]. Activities of these DNazymes are dependent on the elaborate DNA structures for the specific binding of cofactors such as metal ions, hemin, etc. However, there is a great demand to develop DNazymes with straightforward DNA structures, for example, the classic duplex. During a base excision repair (BER) pathway for damaged bases, an abasic site (AP site) can be produced in duplex and it can be then recognized by specific nucleases [11]. Furthermore, the AP site-containing DNAs provide binding cavities for ligands to recognize this site and develop novel sensors [12–15]. We expect that the AP site will functionalize duplex via a simple way for establishing, such as, novel DNazymes.

The photosensitization of DNAs is now attracting much interest as it becomes an alternative method for the treatment of cancers [16–22]. In this aspect, the most investigated DNA structures are G-quadruplexes (G4s) [23–28]. The specific binding of G4s activates photosensitizers with the potential to develop photocatalytic DNazymes for photodynamic therapy. The photosensitizers activated by G4s thus become fluorescent with a resultant long-lived excited state and there is an increased chance of transferring electrons or energy to the dissolved oxygen to produce reactive oxygen species (ROS). However, there are some detrimental factors with this DNzyme which limit its wide applications. Firstly, particularly guanine-rich sequences are required to form the G4 structures. It is well-known that guanine is the most easily oxidized base among all of the bases. Therefore, there exists a tendency to break the G4-based DNazymes by charge transfer between guanine and the excited photosensitizers. Secondly, specific cations (such as K^+) are usually needed

to stabilize the G4 structures. This will confine the G4-based DNAzyme applications to a special circumstance. Thirdly, only macrocyclic compounds (such as porphyrins) are usually used as the G4-binding photosensitizers. There is a great demand for developing variant photosensitizers for expanding photocatalytic DNAzymes.

It has been reported that natural isoquinoline alkaloids (NIAs) can bind with fully matched duplex DNAs (FM-DNAs) with a moderate activity to produce ROS (such as $^1\text{O}_2$) [29], as NIAs exhibit considerable biological activities [30,31]. However, we previously found that NIAs have an obviously enhanced binding with DNAs containing an AP site (AP-DNA) in comparison to FM-DNAs [12]. This opens an avenue to develop duplex-based photocatalytic DNAzymes with an improved activities. In this work, we reported a photocatalytic DNAzyme using the AP site as the active site for the first time.

2. Materials and Methods

Materials and reagents. DNAs (Table 1) were synthesized using TaKaRa Biotechnology Co., Ltd. (Dalian, China) and purified by HPLC (with purity of ~95%). DNA concentrations were measured by first dissolving DNA in pure water and detecting the UV absorbance at 260 nm using extinction coefficients calculated by nearest neighbor analysis. Metal nitrate salts were purchased from Aladdin Reagent Co. (Shanghai, China). Palmatine (PAL), berberine (BER), sanguinarine (SAN), chelerythrine (CHE), and uracil-DNA glycosylase (UDG) were obtained from Sigma Chemical Co. (St. Louis, MO, USA). Coptisine (COP) and jatrorrhizine (JAT) were purchased from Aladdin Reagent Co. (Shanghai, China). Epiberberine (EPI) and worenine (WOR) were obtained from Huicheng Biological Technology Co. (Shanghai, China) and Sichuan Weikeqi Biological Technology Co. (Chengdu, China), respectively. Singlet oxygen sensing green (SOSG) was purchased from Haoran Biotechnology Co., Ltd. (Shanghai, China). LEDs were purchased from Aijia Electronic Technology Co., Ltd. (Xuzhou, China). Other reagents were of analytical grade (Sigma Chemical Co., St. Louis, MO, USA) and used without any purification. Milli-Q water (18.2 M Ω ; Millipore Co, Billerica, MA, USA) was used in all of the experiments.

Table 1. DNA sequences used in this work.

Name	Sequence	Remark
AXA-A	5'-ATGGTGAXAGCAGCG-3' 3'-TACCACTATCGTCGC-5'	X = AP site
AXA-C	5'-ATGGTGAXAGCAGCG-3' 3'-TACCACTCTCGTCGC-5'	X = AP site
AXA-G	5'-ATGGTGAXAGCAGCG-3' 3'-TACCACTGTCGTCGC-5'	X = AP site
AXA-T	5'-ATGGTGAXAGCAGCG-3' 3'-TACCACTTTCGTCGC-5'	X = AP site
FM-DNA	5'-ATGGTGATAGCAGCG-3' 3'-TACCACTATCGTCGC-5'	
AUA-A	5'-ATGGTGAUAGCAGCG-3' 3'-TACCACTATCGTCGC-5'	

Fluorescence and DNAzyme measurements. Fluorescence was measured using a FLSP920 spectrofluorometer (Edinburgh Instruments Ltd., Livingston, UK) at 20 °C, which was equipped with a temperature-controlled circulator (Julabo Labortechnik GmbH, Seelbach, Germany). A quartz cell with a path length of 1 cm was used as the cuvette. Duplex was incubated with ligand for 30 min before fluorescence measurement. For the DNAzyme test, substrate was added to the DNA/ligand solution and the resultant solution was irradiated using an LED source for a desired time with a distance of 13 cm away from the chamber. Control experiments were carried out by checking any of the factors in determining the DNAzyme. If not specified, 20 mM phosphate containing 60 mM K $^+$ at desired pH (PBS) was used as buffer. For UDG experiments, the mixture of AUA-A and PAL in 1 \times UDG reaction buffer was incubated with UDG for the desired time, then PBS was used to adjust

pH to 9.0 before the PAL fluorescence was measured. The substrate was then added into the UDG treated solution, and the light irradiation was applied for the desired time before oxidation product of the substrate was monitored by fluorescence.

Absorption spectra and DNAzyme measurements. Absorption spectra were determined using a UV2550 spectrophotometer (Shimadzu Corp., Kyoto, Japan), equipped with a temperature-controlled circulator (Julabo Labortechnik GmbH, Seelbach, Germany) at 20 °C. 500 μ M substrate containing duplex/PAL or PAL was treated with or without illumination of a blue LED for the desired time before acquiring the absorption spectra.

DNA melting measurements. DNA melting was measured using the UV2550 spectrophotometer (Shimadzu Corp., Kyoto, Japan) but equipped with a TMSPC-8 T_m analysis system in 20 mM PBS buffer (60 mM K^+ , pH 9.0). A micro multi-cell with eight chambers (100 μ L in volume) was used as the cuvette. This system can simultaneously control all chambers with little temperature deviation. The absorbance at 260 nm, as a function of solution temperature, was collected between 5 and 100 °C in 0.5 °C increments, with a 30-s equilibration time applied after each temperature increment. The obtained data were normalized according to the melting fraction α and the melting temperature (T_m) of DNA was acquired by a sigmoidal fitting with $\alpha = 0.5$.

3. Results and Discussion

3.1. Duplex-Based DNAzyme with the AP Site as the Active Site

We have previously reported that PAL, an NIAs can be used as an excellent probe to target the AP site with a turn-on fluorescence response [12]. The interaction of PAL with FM-DNA and AP-DNAs (Table 1) was first investigated by fluorescence. In AP-DNAs, the AP site (X) was flanked by adenines and opposed by any of bases (Y). Thus, we named them AXA-Y (X = AP site; Y = A, C, G, T). Indeed, in comparison with FM-DNA, 100-fold stronger PAL fluorescence was observed when interacting with AXA-T and AXA-C (Figure 1A), while AXA-G and AXA-A caused approximately 80-fold increases in the PAL fluorescence. These results imply that the AP site is just the main binding site of PAL. The observed fluorescence dependency on Y is caused by the cavity size provided by the AP site. The smaller sized pyrimidines (Y = T, C) will provide a larger void than purines (Y = A, G) to better accommodate PAL within the AP site [12]. Therefore, AP-DNAs have the potential to serve as better photocatalytic DNAzymes than FM-DNA, as previously demonstrated for FM-DNA/PAL ensemble for the low efficiency of ROS production.

Amplex Red (AR) was herein used as the substrate of photocatalytic DNAzymes, since its oxidation product (ARox) is fluorescent with a high fluorescence quantum yield [32]. The solutions were irradiated using an LED lamp (15 W) with a central wavelength of around 365 nm, at which PAL can be excited. As shown in Figure 1B, after illumination for 20 min, the characteristic fluorescence band of ARox appears at 580 nm (excitation wavelength at 540 nm), which can be distinguished from the fluorescence band of PAL at around 516 nm. It was observed that the presence of FM-DNA caused no effect on the ARox fluorescence band, while AXA-T otherwise caused a significantly stronger fluorescence response, indicating that AP-DNA played a decisive role in operating the DNAzyme. When the solution was not irradiated, the ARox fluorescence band was not observed even in the presence of AXA-T, indicating that the DNAzyme is driven only by light. The irradiation time-dependent evolution of the ARox fluorescence (Figure 1B) indicates that the photocatalytic kinetics of DNAzyme in the presence of AXA-T is 8.8-fold faster than that obtained with FM-DNA (Figure 1C). In addition, we also examined the effect of the light sources (15 W) including blue LED (450–460 nm), cyan LED (490–500 nm), green LED (520–530 nm), and orange LED (600–610 nm). Only the blue LED was also efficient in driving the DNAzyme (Figure 1D), since it also covers the excitation range of PAL, as indicated in the excitation spectra of Figure 1A. As expected, the DNAzyme activity was directly proportional to the fluorescence behavior of PAL in binding with AP-DNAs (Figure 1E). These results imply that the microenvironment near the AP site directly defines the DNAzyme activity.

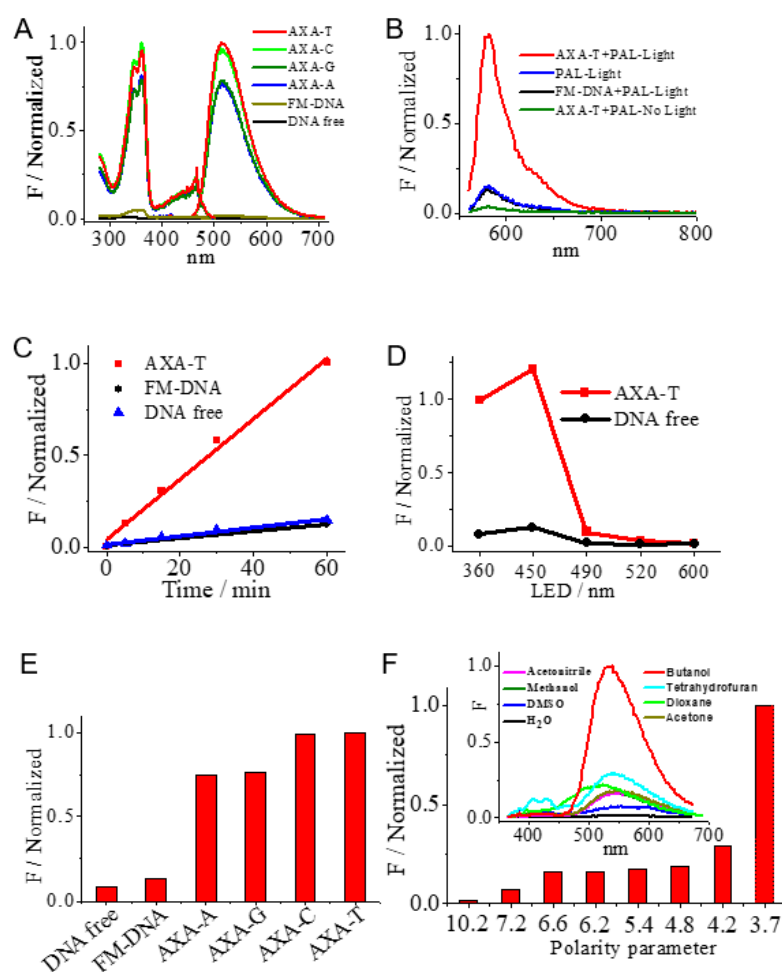


Figure 1. (A) Normalized fluorescence (left) excitation and (right) emission spectra of PAL (2 μM) in the absence and presence of DNAs (1 μM). The excitation spectra were monitored with emission at 515 nm and the emission spectra were obtained with excitation at 360 nm. (B) Normalized emission spectra of AROx produced by photocatalyzed oxidation of AR on different conditions, respectively. Excitation: 540 nm. The solutions were irradiated using a UV LED (15 W) with the central wavelength at 365 nm for 20 min. (C) Evolution of the AROx fluorescence with illumination time. (D) Dependency of the DNAzyme activity on the LED light source. (E) Photocatalyzed AROx fluorescence in the presence of DNAs with irradiation for 20 min. Experimental conditions for (A–E) (20 mM PBS buffer, pH 9.0, 60 mM K^+): DNA at 1 μM ; PAL at 2 μM ; AR at 10 μM . (F) Effect of solvent polarity on PAL fluorescence at 516 nm. Excitation: 365 nm. Experimental conditions: PAL at 10 μM , the organic solvent contains 1% water. Inset: the emission spectra of PAL in organic solvents.

It was expected that the property of the surrounding environment should affect the PAL fluorescence behavior, since PAL becomes emissive when binding with AP-DNA. Therefore, we explored the effect of the solvent polarity on the PAL fluorescence in water, DMSO, methanol, acetonitrile, acetone, dioxane, tetrahydrofuran, and n-butanol (polarity decreases in the order). PAL is soluble in these solvents. As shown in Figure 1F, it seems that the solvents with high polarity decrease the PAL fluorescence. Therefore, in comparison to FM-DNA, the AP site in AP-DNA provides a less polarized environment to accommodate PAL and to activate the PAL fluorescence. These less polarized environment in AP-DNA would favor an energy or electron transfer from the excited PAL to dissolved oxygen to generate ROS [29] that catalytically oxidize the substrate.

To confirm the substrate diversity of the AP-DNA-based DNAzyme, we also tested the substrate of 3,3',5,5'-tetramethylbenzidine (TMB) that is commonly used in the G4/hemin DNAzyme. TMB can be oxidized by the G4/hemin DNAzyme in the presence of H_2O_2

to a colorimetric product (TMBox). As shown in Figure 2A, after 30 min irradiation using the LED lamp, the solution of PAL incubated with AXA-T exhibits the characteristic absorption spectrum of TMBox with absorption bands peaked at 370 nm and 660 nm (curve a), respectively [33]. However, FM-DNA with light irradiation (curve b) and AXA-T without light irradiation (curve d) were totally inefficient to catalyze the TMB oxidation. Furthermore, PAL alone in solution without the presence of DNA cannot also cause the TMBox absorption bands (curve c). The activity of the AP site-switched DNzyme can be clearly observed by the naked eye with a blue appearance for only the solution containing AXA-T under light irradiation (inset of Figure 2). The irradiation time-dependent evolution of the TMBox absorption (Figure 2B) at 660 nm indicates that the photocatalytic kinetics of DNzyme in the presence of AXA-T is 60-fold faster than that obtained with FM-DNA (estimated by the linear response portion). Therefore, this DNzyme can also be operated in a colorimetric manner.

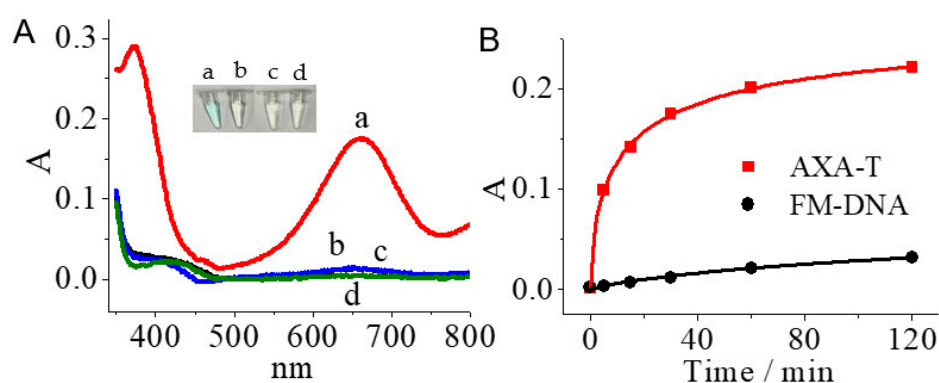


Figure 2. (A) Absorption spectra of photocatalysis oxidation of TMB on conditions of (a) AXA-T+PAL+light illumination, (b) FM-DNA+PAL+light illumination, (c) PAL+light illumination, and (d) AXA-T+PAL+no light illumination, respectively. Illumination with a blue LED (450–460 nm) for 30 min. Inset: photographs of these solutions. (B) Evolution of the TMBox absorption with the illumination time. Experimental conditions for (A,B) (PBS buffer, pH 9.0, 60 mM K⁺): AXA-T and FM-DNA at 3 μ M; PAL at 5 μ M; TMB at 500 μ M.

3.2. Optimized Conditions of DNzyme

AR was used as the substrate to check the factors that affect the DNzyme performance. We found that the DNzyme activity monitored by the ARox fluorescence increased with increasing the solution pH up to 9.0 (Figure 3A), suggesting that alkaline conditions favor the AR oxidation. In addition, increasing in the PAL concentration enhanced the DNzyme activity and the 1:1 concentration ratio of PAL to AXA-T almost saturated the DNzyme activity (Figure 3B). This was caused by the strong binding of PAL with the AP site by a 1:1 mode [12]. The AR concentration-dependent experiments (Figure 3C) demonstrated that 10 μ M AR was enough to maximize the ARox fluorescence for irradiation of 20 min, indicating the high activity of the DNzyme. We also investigated the effect of identity of NIAs on the DNzyme activity. However, JAT, SAN, BER, EPI, COP, WOR, and CHE manifested lower DNzyme activities than PAL (Figure 3D), although they have a similar structure skeleton (Figure 3E). This is consistent with our previous observation that among these NIAs, PAL is the strongest fluorescence emitter when binding with the AP site-containing DNAs.

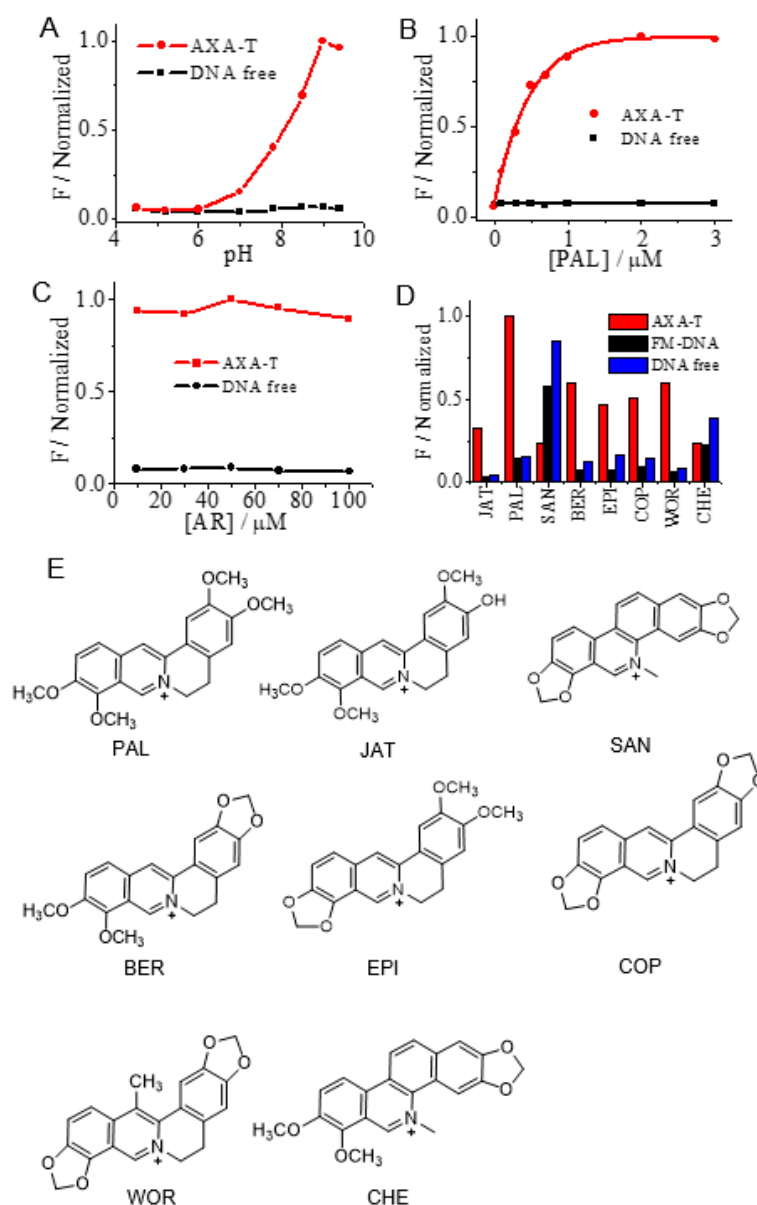


Figure 3. Dependence of the photocatalytic activity of the AP-DNA DNAzyme on factors of: (A) pH; (B) PAL concentration; (C) AR concentration; and (D) identity of NIAs. Experimental conditions: (A) 1 μM AXA-T, 2 μM PAL and 10 μM AR in PBS buffer (60 mM K^+) under the 365 nm LED irradiation for 20 min; (B) 1 μM AXA-T and 10 μM AR in PBS buffer (pH 9.0, 60 mM K^+) under the 365 nm LED irradiation for 20 min; (C) 1 μM AXA-T, and 2 μM PAL in PBS buffer (pH 9.0, 60 mM K^+) under the 365 nm LED irradiation for 20 min; (D) 1 μM DNA, 2 μM NIAs and 10 μM AR in PBS buffer (pH 9.0, 60 mM K^+) under the 365 nm LED irradiation for 20 min. The cases without DNA (DNA free) were used as controls. (E) Structure of NIAs.

3.3. Mechanism of the DNAzyme

According to the above results, we expected that the DNAzyme would work via the pathways of ROS that were produced by energy or electron transfer from the excited PAL to dissolved oxygen. The produced ROS should be singlet oxygen ($^1\text{O}_2$), hydrogen peroxide (H_2O_2), superoxide ($\text{O}_2^{\cdot-}$), or even hydroxyl radicals ($\cdot\text{OH}$) that can subsequently oxidize substrates. To verify this mechanism, we carried out experiments by adding extra ROS scavengers during light irradiating the AXA-T/PAL/AR solution. However, the usage of mannitol and benzoquinone as the $\cdot\text{OH}$ and $\text{O}_2^{\cdot-}$ scavengers [32] did not affect the resultant ARox fluorescence (Figure 4A), indicating that $\cdot\text{OH}$ and $\cdot\text{O}_2^{\cdot-}$ are not the pathways to

drive the DNAzyme. Furthermore, in the absence of AXA-T, PAL, and light irradiation, an extra addition of H_2O_2 did not directly oxidize AR (Figure 4A). This indicates that the DNAzyme cannot photocatalyze the production of H_2O_2 . Interestingly, the presence of tryptophan, a common scavenger for $^1\text{O}_2$ [32,34], lowered the fluorescence of ARox (Figure 4B), indicating that the DNAzyme works via the photoproduction of $^1\text{O}_2$.

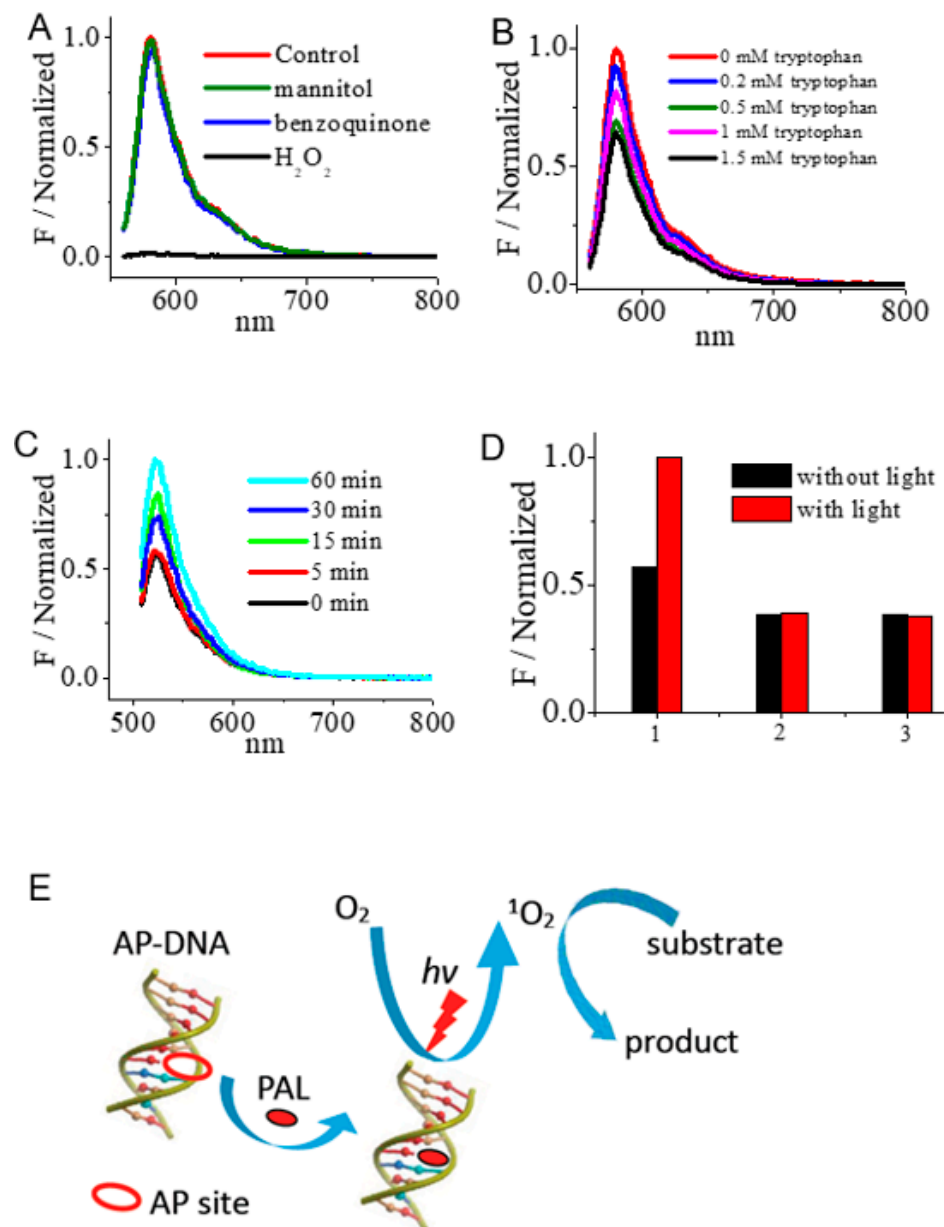


Figure 4. (A) Effect of the addition of benzoquinone and mannitol scavengers (500 μM) on the ARox fluorescence during light irradiation. The ARox fluorescence under normal conditions without these scavengers was used as control. H_2O_2 (500 μM) was directly added into the AR solution without AXA-T and PAL, and no light irradiation was applied. (B) Effect of the addition of different concentration of tryptophan on the ARox fluorescence during light irradiation. Experimental conditions (20 mM PBS buffer, pH 9.0, 60 mM K^+): AXA-T at 1 μM ; PAL at 2 μM ; AR at 10 μM . (C) Fluorescence evolution of the SOSG solution containing AXA-T and PAL upon increasing the light irradiation time. (D) Fluorescence responses at 525 nm under conditions of (1) AXA-T+PAL+SOSG, (2) PAL+SOSG, and (3) SOSG alone under the 60 min light irradiation and without light irradiation, respectively. Experimental conditions for (A–D) (20 mM PBS buffer, pH 9.0, 60 mM K^+): AXA-T at 2 μM ; PAL at 4 μM ; SOSG at 1 μM . (E) Schematic diagram of the AP-DNA-based DNAzyme.

SOSG was used to further verify the $^1\text{O}_2$ pathway. SOSG is a specific probe with a high selectivity for $^1\text{O}_2$ relative to $\cdot\text{OH}$ and $\cdot\text{O}_2^-$ [35]. During light irradiation to the AXA-T/PAL solution, the substrate of AR was replaced by SOSG. Indeed, the characteristic fluorescence band corresponding to the oxidation product of SOSG at 525 nm gradually increased with increment of the light irradiation (Figure 4C). The control experiments (Figure 4D) showed that the light irradiation was necessary to increase the 525 nm band, and the absence of either AXA-T or PAL caused a negligible change on the 525 nm band regardless of whether there was light irradiation or not. These facts clearly indicate that when binding to the AP site in duplex DNA, the excited PAL can transfer the energy to dissolved oxygen to produce ROS $^1\text{O}_2$. Then, the substrate is oxidized by $^1\text{O}_2$ (Figure 4E).

3.4. Stability of the DNAzyme

The DNA melting (T_m) measurements were used to check the DNAzyme stability before and after light irradiation by monitoring the absorption of DNA at 260 nm as a function of the solution temperature. As shown in Figure 5, AXA-T alone in solution had a T_m value of about 40 °C, which was not changed even under the light irradiation for 30 min. Furthermore, with the presence of two equivalent PAL, the T_m value increased to about 46 °C, and the light irradiation for 30 min did not alter this T_m value, indicating that PAL associated with the AP site and the photogenerated $^1\text{O}_2$ did not destroy the duplex structure. The further addition of AR under light irradiation and without light irradiation also kept the AXA-T stability constant (Figure 5).

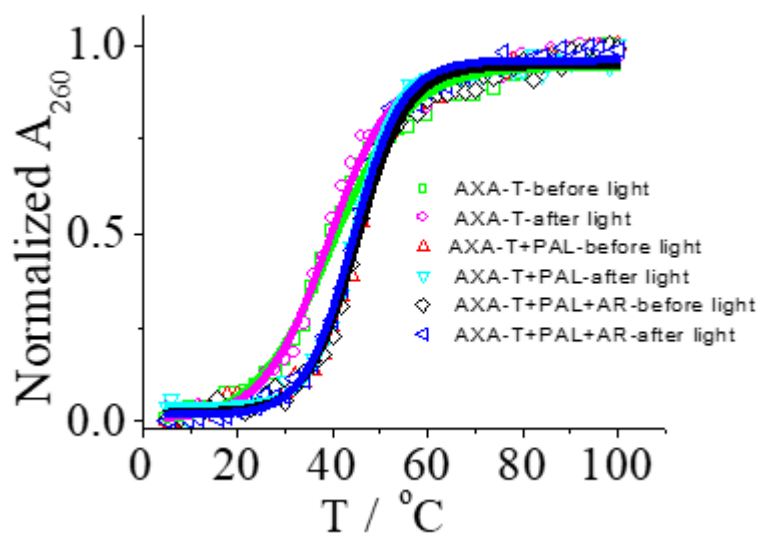


Figure 5. Changes of the AXA-T melting temperature under different conditions. Experimental conditions (PBS buffer, pH 9.0, 60 mM K^+): AXA-T at 2 μM ; PAL at 4 μM ; AR at 10 μM ; and irradiation for 30 min.

3.5. Switch of the DNAzyme Activity Using Cascade UDG

The high DNAzyme activity of AP-DNA, with respect to FM-DNA, provides a means to switch on the DNAzyme activity of FM-DNA using cascade UDG. We designed a duplex of AUA-A with a uracil opposite an adenine (Table 1) in the middle of the duplex. Upon incubation of AUA-A with UDG, a time-dependent fluorescence increase of PAL was observed. The PAL fluorescence was also dependent on the UDG dosage (Figure 6A). These results imply that UDG can remove the uracil from AUA-A to produce the AP site-containing AXA-A in favor of the PAL binding. Thus, the DNAzyme activity of FM-DNA can be imagined using the cascade UDG activation. After the UDG treatment to AUA-A for 3 h, the light irradiation was then applied for AR oxidation and the irradiation time-dependent ARox fluorescence was observed (Figure 6B), indicating the switch of the DNAzyme activity for FM-DNA after the UDG treatment. This will diversify the duplex-based DNAzyme construct.

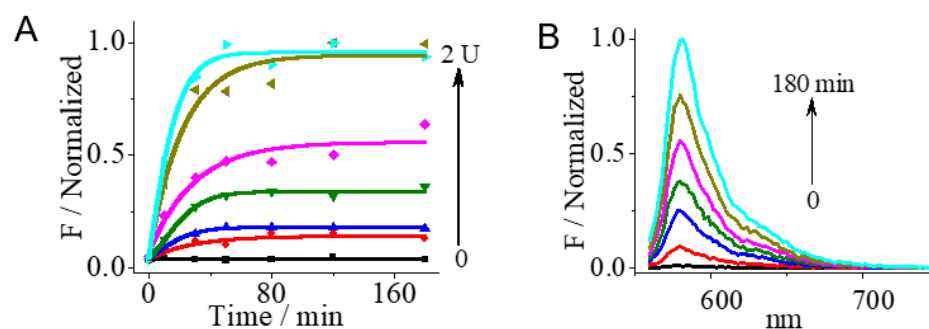


Figure 6. (A) Fluorescence evolution of PAL in the presence of AUA-A upon increasing the the UDG concentration. Experimental conditions (20 mM UDG reaction buffer, pH 8.0): AUA-A at 1 μ M; PAL at 2 μ M. (B) Fluorescence evolution of AR in the presence of AUA-A, PAL and UDG upon increasing the light irradiation time. Experimental conditions: AUA-A at 1 μ M; PAL at 2 μ M; UDG at 1 U/mL. After incubation with UDG in 20 mM reaction buffer (pH 8.0, 60 mM K^+) for 3 h, the solution was adjusted to pH 9.0 using PBS buffer for the light irradiation of different times.

4. Conclusions

In this work, we proposed a duplex-based DNAzyme using an AP site as the active site. PAL, as a photosensitizer, had a strong binding at the AP site. The less polarized environment of the AP site can activate the PAL fluorescence. The excited PAL thus has a chance to transfer energy to dissolved oxygen to generate ROS of 1O_2 . The in situ photogenerated 1O_2 can then catalyze the oxidation of substrates. The DNAzyme has a good stability during operation. In addition, UDG can be used to engineer FM-DNA with an inserted uracil to generate AP-DNA. Therefore, the DNAzyme activity of FM-DNA can be switched by the cascade UDG activation. Since the AP site is always produced in living cells, our work provides a new insight into the duplex-based DNAzyme and promises advanced applications in, for example, photodynamic therapy (PDT), and biosensors.

Author Contributions: Methodology, investigation, and writing—original draft preparation, L.G.; writing—review and editing, R.T.; conceptualization, funding acquisition, and supervision, Y.S. All authors have read and agreed to the published version of the manuscript.

Funding: This work was supported by the Zhejiang Provincial Natural Science Foundation of China (Grant No. LZ20B050001), the Leading Talent Program of Science and Technology Innovation in Zhejiang (Grant No. 2020R52022), the National Natural Science Foundation of China (Grant No. 22274142 and 21675142), and the Independent Designing Scientific Research Project of Zhejiang Normal University (2020ZS0304).

Data Availability Statement: Data is contained within the article.

Conflicts of Interest: The authors declare no conflict of interest.

References

- Ouyang, Y.; O'Hagan, M.P.; Willner, B.; Willner, I. Aptamer-Modified Homogeneous Catalysts, Heterogenous Nanoparticle Catalysts, and Photocatalysts: Functional "Nucleoapzymes", "Aptananozymes", and "Photoaptzymes". *Adv. Mater.* **2023**, *2023*, 2210885. [[CrossRef](#)]
- Lan, T.; Lu, Y. Metal Ion-Dependent DNAzymes and Their Applications as Biosensors. *Met. Ions Life Sci.* **2012**, *10*, 217–248. [[PubMed](#)]
- Yu, Y.; Zhang, Q.; Gao, H.; Yan, C.; Zheng, X.; Yang, T.; Zhou, X.; Shao, Y. Metalloenzyme-Mimic Innate G-quadruplex DNAzymes Using Directly Coordinated Metal Ions as Active Centers. *Dalton Trans.* **2020**, *49*, 13160–13166. [[CrossRef](#)] [[PubMed](#)]
- Zhou, W.; Vazin, M.; Yu, T.; Ding, J.; Liu, J. In Vitro Selection of Chromium-Dependent DNAzymes for Sensing Chromium(III) and Chromium(VI). *Chem. Eur. J.* **2016**, *22*, 9835–9840. [[CrossRef](#)] [[PubMed](#)]
- Santorio, S.W.; Joyce, G.F. Mechanism and Utility of an RNA-Cleaving DNA Enzyme. *Biochemistry* **1998**, *37*, 13330–13342. [[CrossRef](#)] [[PubMed](#)]
- Santorio, S.W.; Joyce, G.F. A General-Purpose RNA-Cleaving DNA Enzyme. *Proc. Natl. Acad. Sci. USA* **1997**, *94*, 4262–4266. [[CrossRef](#)]

7. Yang, X.; Li, T.; Li, B.; Wang, E. Potassium-Sensitive G-Quadruplex DNA for Sensitive Visible Potassium Detection. *Analyst* **2010**, *135*, 71–75. [[CrossRef](#)]
8. Nakayama, S.; Sintim, H.O. Colorimetric Split G-Quadruplex Probes for Nucleic Acid Sensing: Improving Reconstituted DNAzyme's Catalytic Efficiency via Probe Remodeling. *J. Am. Chem. Soc.* **2009**, *131*, 10320–10333. [[CrossRef](#)]
9. Elbaz, J.; Shlyahovsky, B.; Willner, I. A DNAzyme Cascade for the Amplified Detection of Pb²⁺ Ions or L-Histidine. *Chem. Commun.* **2008**, *13*, 1569–1571. [[CrossRef](#)]
10. Li, T.; Wang, E.; Dong, S. Potassium-Lead-Switched G-Quadruplexes: A New Class of DNA Logic Gates. *J. Am. Chem. Soc.* **2009**, *131*, 15082–15083. [[CrossRef](#)]
11. Boiteux, S.; Guillet, M. Abasic Sites in DNA: Repair and Biological Consequences in *Saccharomyces Cerevisiae*. *DNA Repair* **2004**, *3*, 1–12. [[CrossRef](#)] [[PubMed](#)]
12. Wang, Y.; Hu, Y.; Wu, T.; Zhang, L.; Liu, H.; Zhou, X.; Shao, Y. Recognition of DNA Abasic Site Nanocavity by FluoroPhore-Switched Probe: Suitable for All Sequence Environments. *Spectrochim. Acta Part A* **2016**, *153*, 645–650. [[CrossRef](#)] [[PubMed](#)]
13. Yoshimoto, K.; Nishizawa, S.; Minagawa, M.; Teramae, N. Use of Abasic Site-Containing DNA Strands for Nucleobase Recognition in Water. *J. Am. Chem. Soc.* **2003**, *125*, 8982–8983. [[CrossRef](#)] [[PubMed](#)]
14. Rajendran, A.; Zhao, C.; Rajendar, B.; Thiagarajan, V.; Sato, Y.; Nishizawa, S.; Teramae, N. Effect of the Bases Flanking an Abasic Site on the Recognition of Nucleobase by Amiloride. *Biochim. Biophys. Acta* **2010**, *1800*, 599–610. [[CrossRef](#)]
15. Wu, F.; Sun, Y.; Shao, Y.; Xu, S.; Liu, G.; Peng, J.; Liu, L. DNA Abasic Site-Selective Enhancement of Sanguinarine Fluorescence with a Large Emission Shift. *PLoS ONE* **2012**, *7*, e48251. [[CrossRef](#)]
16. Dougherty, T.J.; Gomer, C.J.; Henderson, B.W.; Jori, G.; Kessel, D.; Korbek, M.; Moan, J.; Peng, Q. Photodynamic Therapy. *J. Natl. Cancer Inst.* **1998**, *90*, 889–905. [[CrossRef](#)]
17. Ethirajan, M.; Chen, Y.; Joshi, P.; Pandey, R.K. The Role of Porphyrin Chemistry in Tumor Imaging and Photodynamic Therapy. *Chem. Soc. Rev.* **2011**, *40*, 340–362. [[CrossRef](#)]
18. Rotaru, A.; Mokhir, A. Nucleic Acid Binders Activated by Light of Selectable Wavelength. *Angew. Chem. Int. Ed.* **2007**, *46*, 6180–6183. [[CrossRef](#)]
19. Tørring, T.; Helmig, S.; Ogilby, P.R.; Gothelf, K.V. Singlet Oxygen in DNA Nanotechnology. *Acc. Chem. Res.* **2014**, *47*, 1799–1806. [[CrossRef](#)]
20. Wang, Y.Y.; Dong, Z.; Hu, H.; Yang, Q.; Hou, X.; Wu, P. DNA-Modulated Photosensitization: Current Status and Future Aspects in Biosensing and Environmental Monitoring. *Anal. Bioanal. Chem.* **2019**, *411*, 4415–4423. [[CrossRef](#)]
21. Tardivo, J.P.; Del Giglio, A.; de Oliveira, C.S.; Gabrielli, D.S.; Junqueira, H.C.; Tada, D.B.; Severino, D.; de Fátima Turchiello, R.; Baptista, M.S. Methylene Blue in Photodynamic Therapy: From Basic Mechanisms to Clinical Applications. *Photodiagn. Photodyn. Ther.* **2005**, *2*, 175–191. [[CrossRef](#)] [[PubMed](#)]
22. Lim, S.H.; Thivierge, C.; Nowak-Sliwinska, P.; Han, J.; van den Bergh, H.; Wagnières, G.; Burgess, K.; Lee, H.B. In Vitro and in vivo Photocytotoxicity of Boron Dipyrromethene Derivatives for Photodynamic Therapy. *J. Med. Chem.* **2010**, *53*, 2865–2874. [[CrossRef](#)] [[PubMed](#)]
23. Yin, M.; Li, Z.; Liu, Z.; Ren, J.; Yang, X.; Qu, X. Photosensitizer Incorporated G-Quadruplex DNA-Functionalized Magnetofluorescent Nanoparticles for Targeted Magnetic Resonance/Fluorescence Multimodal Imaging and Subsequent Photodynamic Therapy of Cancer. *Chem. Commun.* **2012**, *48*, 6556–6558. [[CrossRef](#)]
24. Yuan, Q.; Wu, Y.; Wang, J.; Lu, D.; Zhao, Z.; Liu, T.; Zhang, X.; Tan, W. Targeted Bioimaging and Photodynamic Therapy Nanoplatfrom Using an Aptamer-Guided G-Quadruplex DNA Carrier and Near-Infrared Light. *Angew. Chem. Int. Ed.* **2013**, *52*, 13965–13969. [[CrossRef](#)] [[PubMed](#)]
25. Neidle, S. Quadruplex Nucleic Acids as Novel Therapeutic Targets. *J. Med. Chem.* **2016**, *59*, 5987–6011. [[CrossRef](#)]
26. Monchaud, D.; Teulade-Fichou, M.P. A Hitchhiker's Guide to G-Quadruplex Ligands. *Org. Biomol. Chem.* **2008**, *6*, 627–636. [[CrossRef](#)]
27. Liu, Y.C.; Liang, H. Water-soluble Ruthenium (II) Complexes with Chiral 4-(2,3-Dihydroxypropyl)-Formamide Oxoaporphine (FOA): In Vitro and in vivo Anticancer Activity by Stabilization of G-Quadruplex DNA, Inhibition of Telomerase Activity, and Induction of Tumor Cell Apoptosis. *J. Med. Chem.* **2015**, *58*, 4771–4789.
28. Gao, L.; Tong, X.; Ye, T.; Gao, H.; Zhang, Q.; Yan, C.; Yu, Y.; Fei, Y.; Zhou, X.; Shao, Y. G-Quadruplex-Based Photooxidase Driven by Visible Light. *ChenCatChem* **2020**, *12*, 169–174. [[CrossRef](#)]
29. Hirakawa, K.; Hirano, T. The Microenvironment of DNA Switches the Activity of Singlet Oxygen Generation Photosensitized by Berberine and Palmatine. *Photochem. Photobiol.* **2008**, *84*, 202–208. [[CrossRef](#)]
30. Hirakawa, K.; Hirano, T.; Nishimura, Y.; Arai, T.; Nosaka, Y. Dynamics of Singlet Oxygen Generation by DNA-Binding Photosensitizers. *J. Phys. Chem. B* **2012**, *116*, 3037–3044. [[CrossRef](#)]
31. Hirakawa, K.; Nishimura, Y.; Arai, T.; Okazaki, S. Singlet Oxygen Generating Activity of an Electron Donor Connecting Porphyrin Photosensitizer Can Be Controlled by DNA. *J. Phys. Chem. B* **2013**, *117*, 13490–13496. [[CrossRef](#)] [[PubMed](#)]
32. Zhang, X.; Huang, C.; Xu, S.; Chen, J.; Zeng, Y.; Wu, P.; Hou, X. Photocatalytic Oxidation of TMB with The Double Stranded DNA-SYBR Green I Complex for Label-Free and Universal Colorimetric Bioassay. *Chem. Commun.* **2015**, *51*, 14465–14468. [[CrossRef](#)] [[PubMed](#)]
33. Stefan, L.; Denat, F.; Monchaud, D. Insights into How Nucleotide Supplements Enhance the Peroxidase-Mimicking DNAzyme Activity of the G-Quadruplex/Hemin System. *Nucleic Acids Res.* **2012**, *40*, 8759–8772. [[CrossRef](#)]

34. Hu, H.; Zhang, J.; Ding, Y.; Zhang, X.; Xu, K.; Hou, X.; Wu, P. Modulation of the Singlet Oxygen Generation from the Double Strand DNA-SYBR Green I Complex Mediated by T-Melamine-T Mismatch for Visual Detection of Melamine. *Anal. Chem.* **2017**, *89*, 5101–5106. [[CrossRef](#)] [[PubMed](#)]
35. Shi, X.; Fettinger, J.C.; Davis, J.T. Homochiral G-quadruplexes with Ba²⁺ but Not with K⁺: The Cation Programs Enantiomeric Self-Recognition. *J. Am. Chem. Soc.* **2001**, *123*, 6738–6739. [[CrossRef](#)]

Disclaimer/Publisher's Note: The statements, opinions and data contained in all publications are solely those of the individual author(s) and contributor(s) and not of MDPI and/or the editor(s). MDPI and/or the editor(s) disclaim responsibility for any injury to people or property resulting from any ideas, methods, instructions or products referred to in the content.